The 21th Cambridge Workshop on Cool Stars, Stellar Systems, and the Sun
Edited by A. S. Brun, J. Bouvier, P. Petit

Study of the *Gaia* luminosity function of low-mass stars with the Besançon Galaxy Model

Thomas Ravinet[1,2], Nadège Lagarde[2], Céline Reylé[1], Louis Amard[3], Valérie Van Grootel[4]

[1] Université de Franche-Comté, Institut UTINAM, CNRS UMR6213, OSU THETA Franche-Comté-Bourgogne, Observatoire de Besançon, BP 1615, 25010 Besançon Cedex, France
[2] Laboratoire d'astrophysique de Bordeaux, CNRS UMR5804, Bordeaux, France
[3] Département d'Astrophysique/AIM, CEA/IRFU, CNRS/INSU, Univ. Paris-Saclay & Univ. de Paris, 91191 Gif-sur-Yvette, France
[4] Space sciences, Technologies and Astrophysics Research (STAR) Institute, Université de Liège, 19C Allée du 6 Août, 4000 Liège, Belgium

Abstract

Context. The *Gaia* (Early) Data Release 3 provides a large sample of stars with precise parallaxes, distances and photometry from the brightest stars to the stellar-substellar limit. The *Gaia* Catalogue of Nearby Stars permits to have a complete view of the stellar content of the solar neighbourhood.
Aims. Comparing simulations of the stellar content in the solar neighbourhood and the *Gaia* Catalogue of Nearby Stars, we plan to constrain the Initial Mass Function of field stars down to the stellar-substellar limit.
Methods. We construct the luminosity function of the *Gaia* Catalogue of Nearby Stars in the 2MASS J-band. We compare it to luminosity functions from the literature, and show it reproduces features previously observed. Using the Besançon Galaxy Model, we observe the effects of different litterature Initial Mass Functions on simulated luminosity functions. We compare them with the luminosity function of the *Gaia* Catalogue of Nearby Stars in the *Gaia* G-band.
Conclusions. We show that published IMFs do not permit to simulate luminosity functions comparable with the GCNS observed one, particularly for faint stars. Our updated model will allow to constrain the IMF of field stars thanks to *Gaia* data.

1 Introduction

Luminosity functions permit to study the importance, in number density, of the different types of stars in our galaxy. They can be derived from different samples of stars, gathered from clusters and associations or from the field.
Clusters and associations are great environments to link luminosity functions to mass distributions. Their luminosity functions, coupled with evolutionary models and knowing their ages, allow determining their mass functions (Miret-Roig *et al.*, 2019). Young associations can be used to probe the number of brown dwarfs and free-floating planets (Miret-Roig *et al.*, 2022).

It is also possible to study field stars and brown dwarfs to estimate luminosity and mass functions of the galaxy. Kirkpatrick *et al.* (2021) obtained the mass distribution of field brown dwarfs using their spectral types, temperatures and evolutionary models.

The luminosity function of low-mass, main sequence stars, that live billions of years, can be transformed to a mass function through mass-magnitude relationships (Delfosse *et al.*, 2000; Mann *et al.*, 2019), and linked to their Initial Mass Function (IMF), the mass distribution of stars at their birth (Chabrier, 2003; Bastian *et al.*, 2010).

Building field luminosity functions demands to measure distances of objects to evaluate their absolute magnitude. With the *Gaia* mission (Gaia Collaboration, Brown A.G.A *et al.*, 2016) and its Early Data Release 3 (EDR3, Gaia Collaboration, Brown A.G.A *et al.*, 2021), we now have access to high precision parallaxes and photometry. A product of the EDR3, the *Gaia* Catalogue of Nearby Stars (GCNS) (Gaia Collaboration, Smart, R.L. *et al.*, 2021), contains around 330 000 stars within a 100 pc around the Sun, spanning a wide range of spectral types and magnitudes. This new catalogue can be used to assess solar neighbourhood properties with great precision. One important outcome of the GCNS is the determination of its luminosity function, visible on figure 16 of the original article. It allows visualizing various features of the stellar distribution in the solar neighbourhood, that can be put in perspective with the ones observed in luminosity functions from smaller samples, anterior to the GCNS.

In section 2, we use the GCNS crossmatch with the 2MASS survey (Skrutskie *et al.*, 2006) to compute its luminosity function in the J-band, and compare it to ones already published in the literature. Using an updated version of the Besançon Galaxy Model (BGM, Lagarde *et al.*, 2017, 2019), we study the effects of published IMFs on simulated luminosity functions in section 3. In section 4, we expose perspectives of this study.

2 Observed luminosity functions

The GCNS has been used to derive a luminosity function in the *Gaia* G-band, $\phi = \frac{\mathrm{d}N}{\mathrm{d}M_G}$ (Gaia Collaboration, Smart, R.L. *et al.*, 2021). However, published luminosity functions, issued from other surveys, are not expressed in that band. We make use of the crossmatch between the GCNS and 2MASS (Skrutskie *et al.*, 2006) to obtain the $J-$band photometry of 95% of stars in the *Gaia* sample, and to compute a luminosity function in that near-infrared band. To derive the luminosity function of the GCNS in the 2MASS J-band, we fol-

low the procedure from Gaia Collaboration, Smart, R.L. *et al.* (2021). The objects used to construct the luminosity function are selected from the GCNS, from which we removed objects fainter in the G-band than the *Gaia* limiting magnitude map, published along the GCNS. Objects fainter than the 2MASS limiting J-magnitude, $J_{\rm lim} = 15.8$ (Skrutskie *et al.*, 2006) are also rejected.
Then, the contribution of each source to the local stellar density is computed with the $V_{\rm max}$ classical technique (Schmidt, 1968), where $V_{\rm max}$ represents the maximum volume a source could occupy in the survey. It permits to correct for the density contribution of faint stars, that are not detected up to the 100 pc distance limit of the GCNS. Computing it requires calculating $d_{\rm max}$, the maximal distance at which a star with absolute magnitude M_J could be seen, and still be included in the survey.

$$d_{\rm max} = \min\left(10^{\frac{J_{\rm lim}-M_J}{5}+1}; 100\,{\rm pc}\right)$$

In order to take into account the decrease in stellar density with increasing distance above the galactic plane, we use the so called generalized form of $V_{\rm max}$ defined by Tinney *et al.* (1993) as follows:

$$V_{\rm max} = \Omega\frac{H^3}{|\sin(b)|^3}\left[2-(\xi^2+2\xi+2)\exp(-\xi)\right]$$

with $\xi = \frac{d_{\rm max}\sin|b|}{H}$, Ω the probed solid angle of the survey (4π for an all-sky survey), $H = 365\,{\rm pc}$ the thin-disc scale height, b the galactic latitude.

The luminosity function is then computed per 0.25 absolute magnitude bin, in which we sum the density contribution of each source $\phi = \sum_{\rm bin}\frac{1}{V_{\rm max}}$.

Figure 1 presents the GCNS J-band luminosity function, in blue. Its accuracy is achieved thanks to *Gaia* precise astrometry and GCNS completeness, leading to a 1-σ error of $\sim 1\%$. It is plotted together with four luminosity functions from the literature:

- Bochanski *et al.* (2010) used SDSS DR6 to compile a luminosity function with spectrophotometric distances, for stars with a mass within $0.1 - 1\,M_\odot$ located in a $4\times4\times4\,{\rm pc}^3$ volume around the Sun. GCNS and Bochanski *et al.* (2010) luminosity functions peak at $M_J = 8$. According to Kroupa & Tout (1997), that maximum is caused by the shape of the mass-magnitude relationship, for stars with masses near $0.3M_\odot$.

- Cruz *et al.* (2007) used a sample of 99 late-M and L dwarfs, within 20 pc, selected through their colours. As well as the GCNS luminosity function, it shows a decrease in density at the stellar-substellar transition.

- Bardalez Gagliuffi *et al.* (2019) compiled a 25 pc sample of 306 M7-L5 dwarfs, most of them confirmed spectroscopically, to build a luminosity function from that volume-limited sample. Like Cruz *et al.* (2007) luminosity function, it decreases at the stellar-substellar transition. It agrees within 3-σ with the GCNS luminosity function but has a higher value for stars in the $12 < M_J < 14$ range. The difference may be linked to an incompleteness in the GCNS for faint objects: the survey is expected to be incomplete for objects with spectral type later than M7, and is estimated to be incomplete below 25 pc for brown dwarfs later than L3 (see figure 26 of Gaia Collaboration, Smart, R.L. *et al.*, 2021). Thus, magnitude bins fainter than $M_J \sim 11$ are expected to be incomplete.

- Reylé *et al.* (2010) computed a magnitude-limited luminosity function for ultracool L and T dwarfs from the Canada-France-Brown-Dwarf Survey (Delorme *et al.*, 2008).The GCNS luminosity function shares common magnitude bins with it, between $M_J = 13.75$ and 15.25. Despite the incompleteness in that magnitude range, we observe that the GCNS luminosity function, on average, seems to reproduce the increase in density of brown dwarfs that was observed in Reylé *et al.* (2010). The difference between the Reylé *et al.* (2010) luminosity function and the GCNS luminosity function might be caused by the GCNS incompleteness.

The GCNS luminosity function reproduces the behaviour of previously published luminosity functions in an homogeneous way. The luminosity function reaches a minimum that has been highlighted by Gaia Collaboration, Smart, R.L. *et al.* (2021) and interpreted as the substellar-stellar transition. This was also predicted from earlier simulations performed by Burgasser (2004) and Allen *et al.* (2005), and can be explained by the different evolutionary process for stars and brown dwarfs. Stars, once stabilized on the main sequence, do not show strong variation in their luminosity during their lifetime, while brown dwarfs cool down and become fainter, as they don't fuse their hydrogen. Thus, they populate higher magnitude ranges as they age.

3 Simulations of the luminosity function

In this study, we aim to simulate the GCNS luminosity function, and to study its dependence to the IMF. We use the BGM (e.g. Lagarde *et al.*, 2017, 2019) to mimic the stellar content of the GCNS.

3.1 Ingredients of the Besançon Galaxy Model

The BGM is a stellar population synthesis code. It relies on different assumptions and models to simulate the stellar content of a zone of the sky.

It synthetizes four stellar populations : a thin disk, a thick disk, a bar, and a halo. Each population have a different density distribution within the galactic disk. Star initial masses of each population are drawn from an IMF, that as the form of a broken power-law $\Psi(m) = \frac{{\rm d}N}{{\rm d}m} \propto m^{-\alpha}$. Their ages τ are distributed using a Star Formation History $SFH \propto \exp -0.12\times\tau$ from Aumer & Binney (2009). Metallicity and $[\alpha/Fe]$ distributions are also taken into account (see Lagarde *et al.*, 2019). Stars astrophysical parameters (current mass, $T_{\rm eff}$, $\log g$, radius, luminosity) are obtained through interpolations in stellar evolutionary models.

Stellar evolutionary models computed with the code STAREVOL (e.g. Lagarde *et al.*, 2012 and Amard *et al.*, 2019) are used to simulate characteristics of stars more massive than $0.2M_\odot$. We implemented the CLES evolutionary models (Fernandes *et al.*, 2019, Van Grootel, V, priv. comm.) to simulate objects with a mass within $\sim 0.08 - 0.13M_\odot$. Stellar masses between $0.13M_\odot < m < 0.2M_\odot$ are not covered by the implemented stellar evolutionary models yet, and will

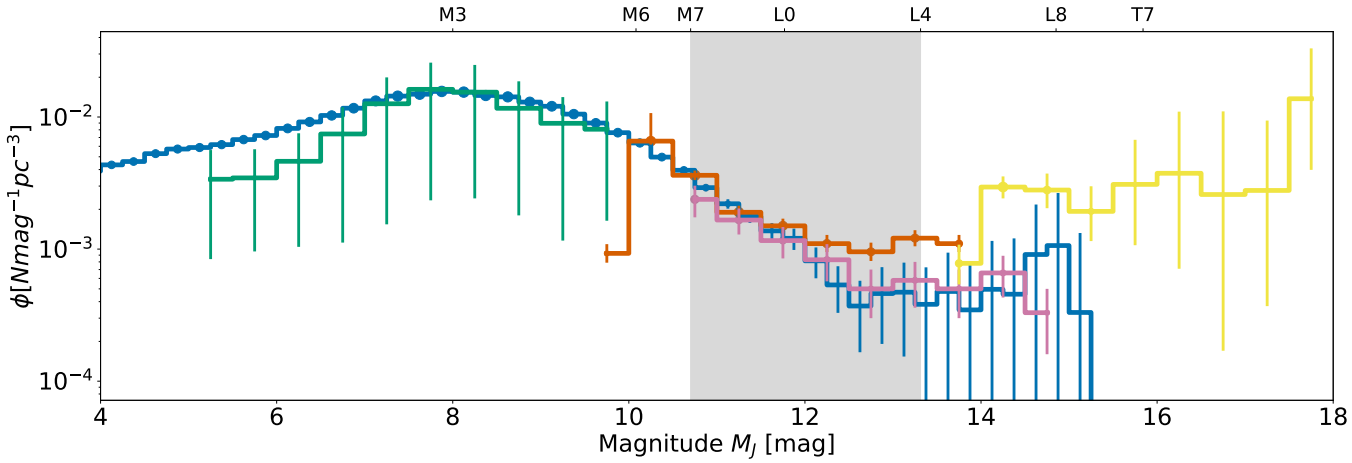

Figure 1: Luminosity functions observed in the J-band from the GCNS, derived in this study (blue, 1-σ Poisson error bars), Bochanski *et al.* (2010) (orange, min-max error bars), Bardalez Gagliuffi *et al.* (2019) (green, 1-σ Poisson error bars), Cruz *et al.* (2007) (red, 1-σ Poisson error bars) and Reylé *et al.* (2010) (purple, 2-σ Bayesian error bars). The grey-shaded area is indicative to the stellar-substellar transition for field stars. Spectral types are indicative, and issued from Filippazzo *et al.* (2015).

be added in a future work. Stellar atmosphere models (Allard *et al.*, 2013) are then used to define the colours of stars generated in different magnitude systems. We also apply a diffuse extinction of $0.7\,\mathrm{mag/kpc}$. Binary stars are merged to the same source if they appear closer than the *Gaia* EDR3 spatial resolution of 0.18 arsec[1].

3.2 Impacts of the IMF on luminosity functions

Assuming four different IMFs, we simulate the stellar content of a 100 pc sphere around the Sun. The slopes of the four IMFs are given in table 1. Three of them were found in the literature (Sollima, 2019; Mor *et al.*, 2019; Kroupa, 2008), while the fourth is a composite IMF currently in use in the BGM, inspired from Kroupa (2008) for low mass stars and from Mor *et al.* (2019) for the more massive stars.

Luminosity functions are computed from BGM catalogues following the same procedure as developed in section 2. The limiting G-magnitude we use is between 18.5 and 20.7, depending on the sky direction, as given in Gaia Collaboration, Smart, R.L. *et al.* (2021) (see their figure 6). As this study does not focus on the local density of stars, simulated luminosity functions are arbitrarily normalized to match the observed GCNS density at $M_G = 8$, corresponding to stars with a mass of $\sim 0.5\,M_\odot$. We compare the effects of the IMFs on simulated luminosity functions in the $G-$band on figure 2, on which we also show the GCNS luminosity function.

We note the following variations between simulations and the observation of the luminosity function :

- The shape of the density distribution between $M_G = 4$ and $M_G = 8$, corresponding to stars with masses between $\sim 1.5M_\odot$ and $\sim 0.5M_\odot$, is well represented by IMFs from Sollima (2019) and Mor *et al.* (2019), that are inferred from *Gaia* DR2 data, as well as by our composite IMF. The Kroupa (2008) IMF is too steep below $0.5M_\odot$, and fail to reproduce that part of the luminosity function.
- The maximum of the observed luminosity function is located around $M_G = 11$, and its origin is described in section 2. Kroupa (2008), Sollima (2019) and our composite IMFs permit to simulate a luminosity function matching this maximum. The IMF proposed by Mor *et al.* (2019) is estimated from a sample limited to bright sources with $G < 12$. As it contains only a few low-mass stars, it fails to constrain the IMF for stars less massive than $0.5M_\odot$. Thus, the simulation using this IMF do not produce a luminosity function matching the observed maximum, and underestimate the density of low-mass stars.
- The luminosity functions show a slow decrease of density between the $M_G = 11$ and $M_G = 15.5$. The simulated luminosity functions do not match the observed one in that magnitude range.
- The drop that is visible at $M_G = 15.5$ in all simulated luminosity functions is due to the current mass-limit in

Table 1: The different IMF slopes used in figure 2.

Source	IMF slopes $\Phi(m) \propto m^{-\alpha}$	
Kroupa (2008)	1.30	if $m < 0.5\,M_\odot$
	2.30	if $m > 0.5\,M_\odot$
Mor *et al.* (2019)	-0.44	if $m < 0.5\,M_\odot$
	1.35	if $0.5\,M_\odot < m < 1.53\,M_\odot$
	2.53	if $m > 1.53\,M_\odot$
Sollima (2019)	1.34	if $m < 1\,M_\odot$
	2.68	if $m > 1\,M_\odot$
Composite IMF	1.30	if $m < 1.53\,M_\odot$
	2.50	if $m > 1.53\,M_\odot$

[1] https://gea.esac.esa.int/archive/documentation/GDR3/Gaia_archive/chap_datamodel/sec_dm_main_source_catalogue/ssec_dm_gaia_source.html

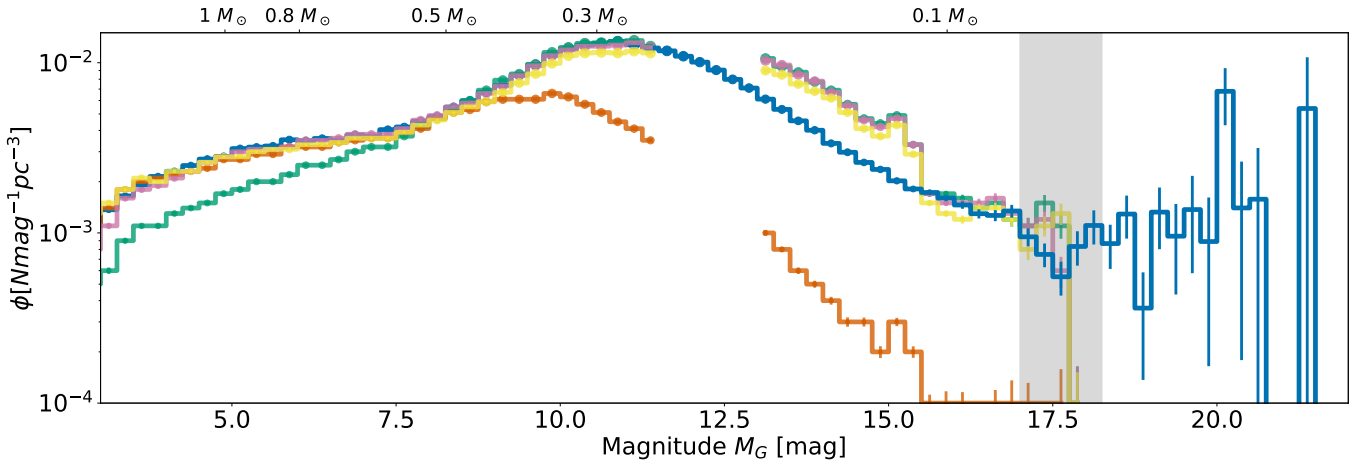

Figure 2: Observed GCNS luminosity function from Gaia Collaboration, Smart, R.L. *et al.* (2021) (blue), compared to BGM synthetic luminosity functions issued from IMFs of Kroupa (2008) (green), Mor *et al.* (2019) (orange), Sollima (2019) (pink) and this study (yellow). Masses are indicative, and not to be taken as a mass-magnitude relation.The grey-shaded area is interpreted as the stellar-substellar transition for field stars (see text).

the BGM evolutionary models. The faintest part of the luminosity function should be populated by light (with $M \lesssim 0.08 M_\odot$) and cold ($T < 2000K$) stars and brown dwarfs, that are not yet implemented in the BGM.

4 Ongoing work and perspectives

The GCNS permits to have a clear view on the stellar content of the solar neighbourhood. We used it and its cross-match with the 2MASS survey (Skrutskie *et al.*, 2006) to obtain the luminosity function of the solar neighbourhood in 2MASS J-band. While compared to published luminosity functions, the latter reproduces their density estimations up to the GCNS completeness limit, at the stellar-substellar transition. Beyond that point, the GCNS luminosity function reproduces, on average, trends that were previously observed. As it spans a wide range of magnitude and spectral types, the GCNS luminosity function is a critical observation that will permit to study homogeneously stars, from the more massive giants to the very low-mass stars.

We have updated the BGM in order to simulate stellar populations properties up to the substellar limit, by integrating new stellar evolutionary models (Amard *et al.* 2019 and Fernandes *et al.* 2019) and recent stellar atmosphere models (Allard *et al.*, 2013).

Using the BGM, we discussed the effects of different published IMF on simulated luminosity functions, that were compared to the GCNS luminosity function. The ones that were computed from *Gaia* DR2 samples (Mor *et al.*, 2019; Sollima, 2019) can accurately reproduce the observed density of stars in the $1.5 - 0.5 M_\odot$ mass range. However, discrepancies are found for less massive stars. Indeed, comparisons with the GCNS content show that the number of low-mass stars is incorrectly estimated by simulations.

In an ongoing work, we will study the different parameters that can influence the luminosity function, in order to constrain the IMF of very low mass stars and brown dwarfs. This implies to further develop the BGM so that it can simulate the properties of these stars below the stellar-brown dwarf limit.

These updates, combined with *Gaia* data, will allow constraining the number of brown dwarfs in the solar neighbourhood. The BGM will then be a crucial tool to study the future deep surveys such as Euclid and LSST, in which many cool brown dwarfs will be observed.

5 Acknowledgements

This research has been supported by the Centre National d'Études Spatiales (CNES) PhD grant 2021-262, and a PhD grant from the Région Bourgogne-Franche-Comté. Simulations have been executed on computers from the UTINAM Institute of the Université de Franche-Comté, supported by the Région de Franche-Comté and Institut des Sciences de l'Univers (INSU). T.R., C.R., and N.L. acknowledge financial support from the "Programme National de Physique Stellaire" (PNPS) and the "Programme National de Cosmologie et Galaxie" (PNCG) of CNRS/INSU, France. This work has made use of data from the European Space Agency (ESA) mission *Gaia* (https://www.cosmos.esa.int/gaia), processed by the *Gaia* Data Processing and Analysis Consortium (DPAC, https://www. cosmos.esa.int/web/gaia/dpac/consortium). It also used packages from Astropy Collaboration *et al.* (2022) and all packages it is built on.

References

Allard, F., Homeier, D., Freytag, B., Schaffenberger, W., & Rajpurohit, A. S. 2013, Memorie della Societa Astronomica Italiana Supplementi, 24, 128. ISSN 0037-8720. ADS Bibcode: 2013MSAIS..24..128A.

Allen, P. R., Koerner, D. W., Reid, I. N., & Trilling, D. E. 2005, The Astrophysical Journal, 625, 385. ISSN 0004-637X. ADS Bibcode: 2005ApJ...625..385A.

Amard, L., Palacios, A., Charbonnel, C., Gallet, F., Georgy, C., *et al.* 2019, Astronomy and Astrophysics, 631, A77. ISSN 0004-6361.

Astropy Collaboration, Price-Whelan, A. M., Lim, P. L., Earl, N., Starkman, N., *et al.* 2022, The Astrophysical

Journal, 935, 167. ISSN 0004-637X. ADS Bibcode: 2022ApJ...935..167A.

Aumer, M. & Binney, J. J. 2009, Monthly Notices of the Royal Astronomical Society, 397, 1286. ISSN 0035-8711. ADS Bibcode: 2009MNRAS.397.1286A.

Bardalez Gagliuffi, D. C., Burgasser, A. J., Schmidt, S. J., Theissen, C., Gagné, J., *et al.* 2019, The Astrophysical Journal, 883, 205. ISSN 0004-637X. ADS Bibcode: 2019ApJ...883..205B.

Bastian, N., Covey, K. R., & Meyer, M. R. 2010, Annual Review of Astronomy and Astrophysics, vol. 48, p.339-389, 48, 339. ISSN 0066-4146.

Bochanski, J. J., Hawley, S. L., Covey, K. R., West, A. A., Reid, I. N., *et al.* 2010, The Astronomical Journal, 139, 2679. ISSN 0004-6256. ADS Bibcode: 2010AJ....139.2679B.

Burgasser, A. J. 2004, The Astrophysical Journal Supplement Series, 155, 191. ISSN 0067-0049. ADS Bibcode: 2004ApJS..155..191B.

Chabrier, G. 2003, Publications of the Astronomical Society of the Pacific, 115, 763. ISSN 0004-6280. ADS Bibcode: 2003PASP..115..763C.

Cruz, K. L., Reid, I. N., Kirkpatrick, J. D., Burgasser, A. J., Liebert, J., *et al.* 2007, The Astronomical Journal, 133, 439. ISSN 0004-6256. ADS Bibcode: 2007AJ....133..439C.

Delfosse, X., Forveille, T., Ségransan, D., Beuzit, J.-L., Udry, S., *et al.* 2000, Astronomy and Astrophysics, v.364, p.217-224 (2000), 364, 217. ISSN 0004-6361.

Delorme, P., Willott, C. J., Forveille, T., Delfosse, X., Reylé, C., *et al.* 2008, Astronomy and Astrophysics, 484, 469. ISSN 0004-6361.

Fernandes, C. S., Van Grootel, V., Salmon, S. J. A. J., Aringer, B., Burgasser, A. J., *et al.* 2019, The Astrophysical Journal, 879, 94. ISSN 0004-637X. ADS Bibcode: 2019ApJ...879...94F.

Filippazzo, J. C., Rice, E. L., Faherty, J., Cruz, K. L., Van Gordon, M. M., *et al.* 2015, The Astrophysical Journal, 810, 158. ISSN 0004-637X. ADS Bibcode: 2015ApJ...810..158F.

Gaia Collaboration, Brown A.G.A, Vallenari, A., Prusti, T., de Bruijne, J. H. J., Babusiaux, C., *et al.* 2021, Astronomy and Astrophysics, 649, A1. ISSN 0004-6361.

Gaia Collaboration, Brown A.G.A, Vallenari, A., Prusti, T., de Bruijne, J. H. J., Mignard, F., *et al.* 2016, Astronomy and Astrophysics, 595, A2. ISSN 0004-6361.

Gaia Collaboration, Smart, R.L., Sarro, L. M., Rybizki, J., Reylé, C., Robin, A. C., *et al.* 2021, Astronomy and Astrophysics, 649, A6. ISSN 0004-6361.

Kirkpatrick, J. D., Gelino, C. R., Faherty, J. K., Meisner, A. M., Caselden, D., *et al.* 2021, The Astrophysical Journal Supplement Series, 253, 7. ISSN 0067-0049. ADS Bibcode: 2021ApJS..253....7K.

Kroupa, P. 2008, 390, 3. Conference Name: Pathways Through an Eclectic Universe Place: eprint: arXiv:0708.1164 ADS Bibcode: 2008ASPC..390....3K.

Kroupa, P. & Tout, C. A. 1997, Monthly Notices of the Royal Astronomical Society, 287, 402. ISSN 0035-8711. ADS Bibcode: 1997MNRAS.287..402K.

Lagarde, N., Decressin, T., Charbonnel, C., Eggenberger, P., Ekström, S., *et al.* 2012, Astronomy and Astrophysics, 543, A108. ISSN 0004-6361.

Lagarde, N., Reylé, C., Robin, A. C., Tautvaišienė, G., Drazdauskas, A., *et al.* 2019, Astronomy and Astrophysics, 621, A24. ISSN 0004-6361.

Lagarde, N., Robin, A. C., Reylé, C., & Nasello, G. 2017, Astronomy and Astrophysics, 601, A27. ISSN 0004-6361.

Mann, A. W., Dupuy, T., Kraus, A. L., Gaidos, E., Ansdell, M., *et al.* 2019, The Astrophysical Journal, 871, 63. ISSN 0004-637X. ADS Bibcode: 2019ApJ...871...63M.

Miret-Roig, N., Bouy, H., Olivares, J., Sarro, L. M., Tamura, M., *et al.* 2019, Astronomy and Astrophysics, 631, A57. ISSN 0004-6361.

Miret-Roig, N., Bouy, H., Raymond, S. N., Tamura, M., Bertin, E., *et al.* 2022, Nature Astronomy, 6, 89. ISSN 2397-3366. Number: 1 Publisher: Nature Publishing Group.

Mor, R., Robin, A. C., Figueras, F., Roca-Fàbrega, S., & Luri, X. 2019, Astronomy and Astrophysics, 624, L1. ISSN 0004-6361.

Reylé, C., Delorme, P., Willott, C. J., Albert, L., Delfosse, X., *et al.* 2010, Astronomy and Astrophysics, 522, A112. ISSN 0004-6361.

Schmidt, M. 1968, The Astrophysical Journal, 151, 393. ISSN 0004-637X. ADS Bibcode: 1968ApJ...151..393S.

Skrutskie, M. F., Cutri, R. M., Stiening, R., Weinberg, M. D., Schneider, S., *et al.* 2006, The Astronomical Journal, 131, 1163. ISSN 0004-6256. ADS Bibcode: 2006AJ....131.1163S.

Sollima, A. 2019, Monthly Notices of the Royal Astronomical Society, 489, 2377. ISSN 0035-8711. ADS Bibcode: 2019MNRAS.489.2377S.

Tinney, C. G., Reid, I. N., & Mould, J. R. 1993, The Astrophysical Journal, 414, 254. ISSN 0004-637X. ADS Bibcode: 1993ApJ...414..254T.